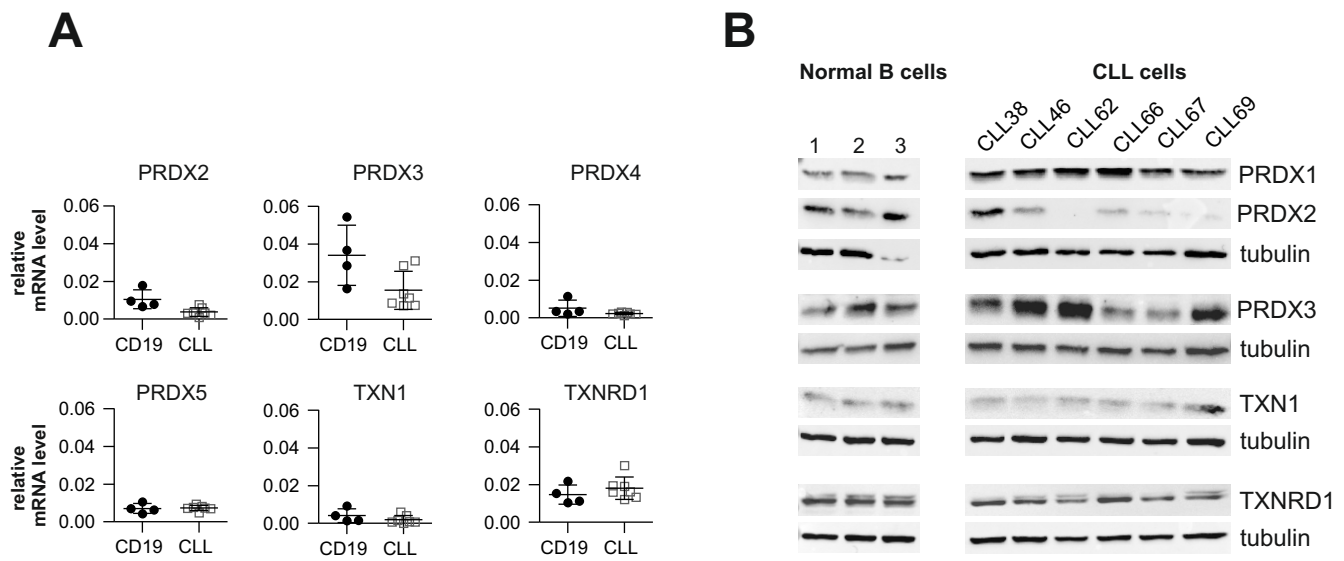
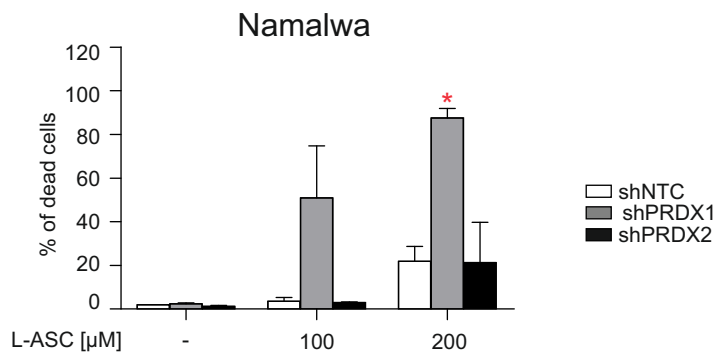


**Supplementary Figure 1. TXN system inhibition sensitizes malignant B-cell-derived cell lines to L-ASC.**

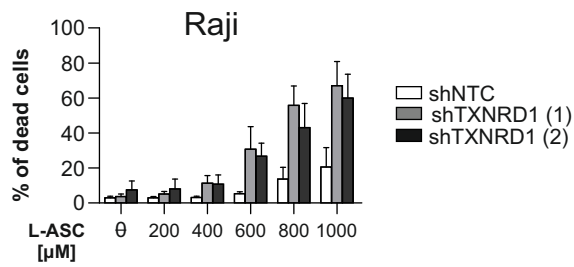
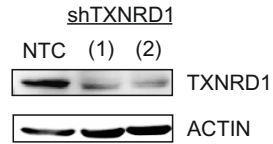
**A.** Raji or Mec-1 cells were incubated for 48 h with L-ASC and SK053 at indicated concentrations added alone or in combination. To assess viability, the cells were stained with propidium iodide (PI) and analyzed by flow cytometry. The results are shown as means of three independent experiments + SD. **B.** Raji cells were incubated 48 h with L-ASC and buthionine sulphoximine (BSO), the inhibitor of glutathione synthesis, at indicated concentrations added alone or in combination. To assess viability, the cells were stained with PI and analyzed by flow cytometry. Bars indicate means of two independent experiments + SD. The statistical significance in **A.** and **B.** was evaluated using 1-way ANOVA test with Tukey's correction in L-ASC only groups and the corresponding combinations with SK053 or BSO. Significant differences are indicated: \*\* $p < 0.01$ , \*\*\*\* $p < 0.0001$ .



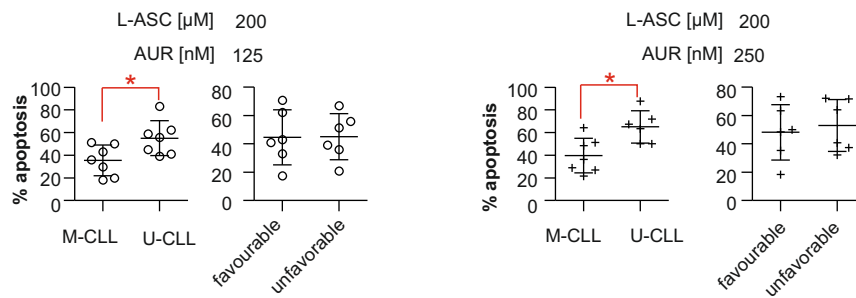
**Supplementary Figure 2. Expression of TXN system antioxidant enzymes in primary CLL and in normal B-cells at mRNA (A) and protein (B) levels. A.** The mRNA levels of the enzymes in normal (CD19<sup>+</sup> cells from peripheral blood of healthy donors, n=4) and malignant (primary CLL, n=7) B-cells were assessed by qPCR, using RPL29 as a reference gene. The results are shown as means  $\pm$ SD and statistical significance was assessed with unpaired *t* test. **B.** Immunoblotting of total protein lysates prepared from blood-derived B-cells of CLL patients (CLL, n=6) or healthy donors (normal B-cells, n=3).



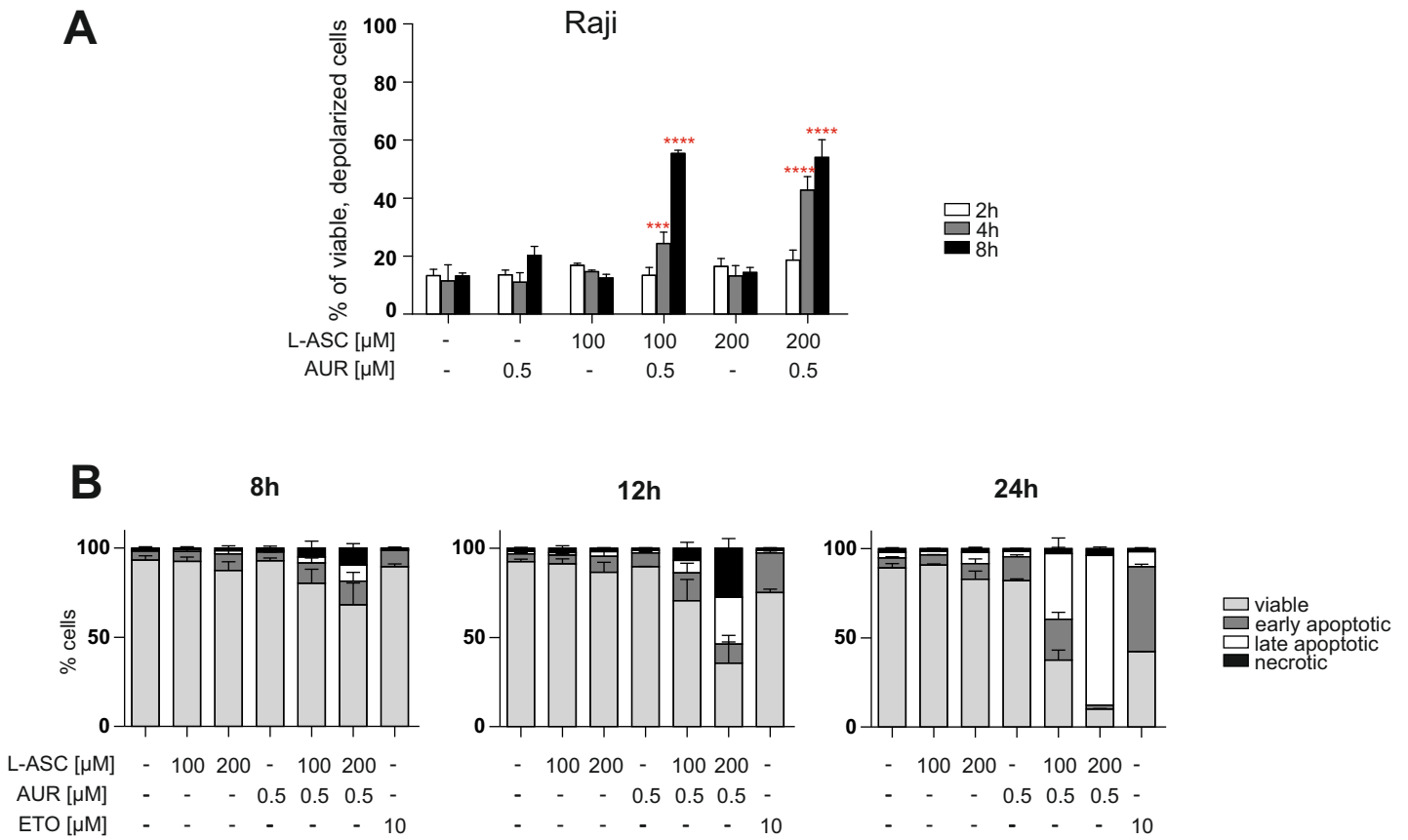
**Supplementary Figure 3. Downregulation of PRDX1 sensitizes Namalwa cells to L-ASC.** Namalwa cells with shRNA-mediated downregulation of PRDX1 or PRDX2 were obtained as described previously [6]. The cells were incubated with L-ASC at indicated concentrations for 48 h. Then, the cells were stained with PI and viability was assessed by flow cytometry. Bars indicate means of two independent experiments + SD. Statistical significance between control cells (shNTC) and cells with PRDX1 and PRDX2 knockdown for each L-ASC concentration was assessed using 1-way ANOVA with Tukey's post-hoc test; \* $p < 0.05$ .

**A****B**

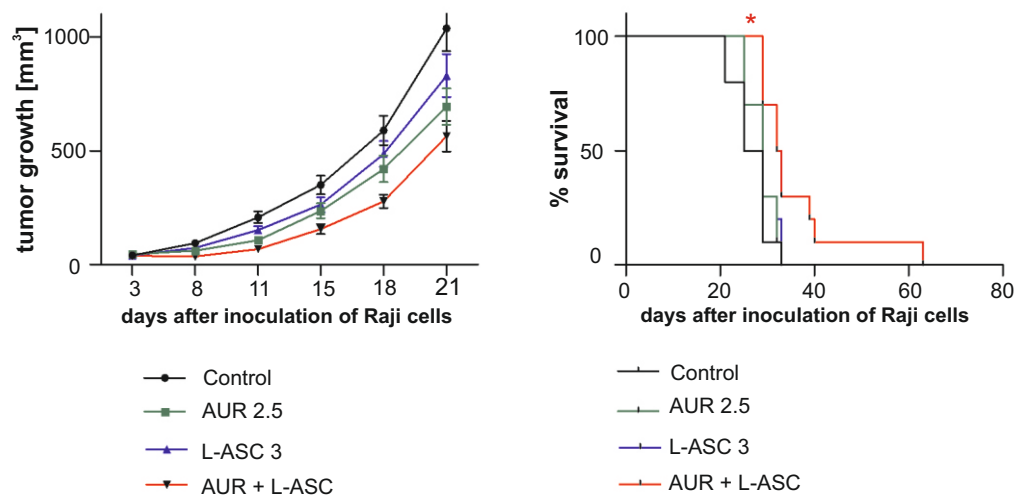
**Supplementary Figure 4. Knockdown of TXNRD1 sensitizes Raji cells to L-ASC.** **A.** Raji cells expressing two different, TXNRD1-specific shRNAs (shTXNRD1 (1) and (2)) and Raji cells expressing non-targeting shRNA (shNTC) were incubated for 48 h with L-ASC at indicated concentrations. To assess their viability, the cells were stained with PI and analyzed by flow cytometry. Results are shown as means of three independent experiments + SEM. **B.** Western blot analysis of the levels of TXNRD1 in total protein lysates of Raji-shTXNRD1 (1), (2), and Raji-shNTC cells.



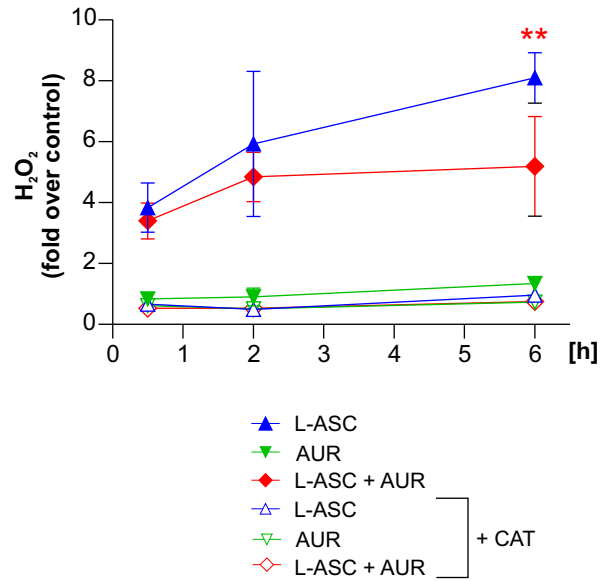
**Supplementary Figure 5. Sensitivity to AUR+L-ASC-induced apoptosis in prognostic subsets of CLL.** CLL prognostic subsets were defined by the *IGHV* gene mutation status (U-CLL – unmutated *IGHV*, n=7, M-CLL – mutated *IGHV*, n=7) or cytogenetic risk group (unfavorable prognosis refers to patients with del 11q or del 17p, n=6 patients, favorable to del 13q and trisomy, n=6 patients). The percentage of apoptotic cells was calculated according to the following formula:  $[(\% \text{ apoptotic cells in a group treated with L-ASC+AUR} - \% \text{ apoptotic cells in a control group}) / \% \text{ apoptotic cells in a group treated with L-ASC+AUR}] \times 100$ . Means  $\pm$  SEM, statistical significance was determined with Mann-Whitney test, \*p<0.05.



**Supplementary Figure 6. A. L-ASC and AUR trigger depolarization of mitochondria and apoptosis in Raji cells. A.** Raji cells were exposed to AUR, L-ASC and their combination at indicated concentrations. Changes in mitochondrial potential were measured at indicated time points. Results are presented as percentage of viable, depolarized cells. The bars indicate mean + SD from three independent experiments. Differences between experimental groups and DMSO-treated control for each time point were assessed by ANOVA with Dunnett's post-hoc test; \*\*\* $p < 0.001$ , \*\*\*\* $p < 0.0001$  **B.** Raji cells were incubated with AUR and L-ASC as single agents and combination of both at indicated concentrations. Cells exposed to 10  $\mu$ M of etoposide (ETO) served as a positive control. Cells were collected at indicated time points, stained with annexin V/ PI and analysed by flow cytometry. Data are shown as percentage of viable, apoptotic and necrotic cells, means + SD from two independent repeats.

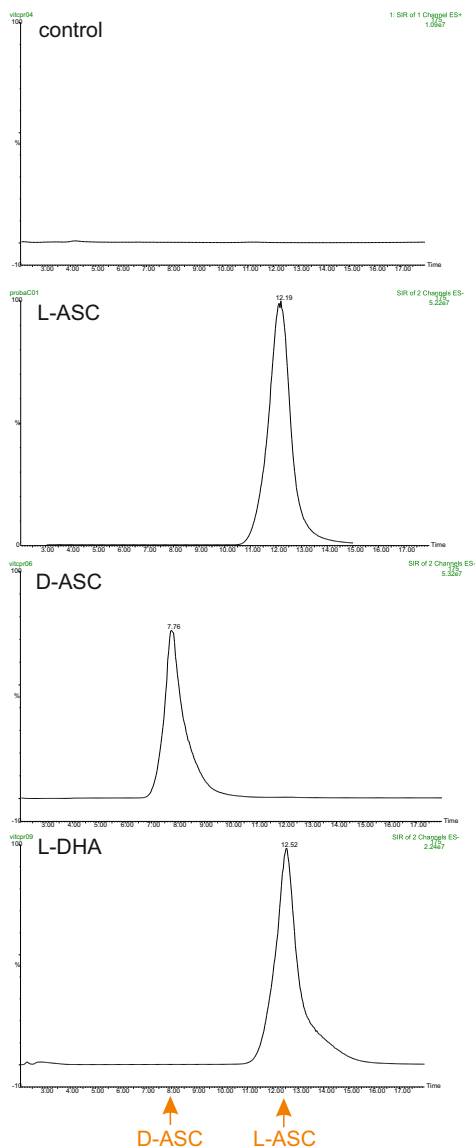


**Supplementary Figure 7. AUR enhances L-ASC antitumor activity *in vivo*.** BALB/c SCID mice were inoculated s.c. with  $1 \times 10^6$  Raji cells in 50% Matrigel on the flank of the mice. Two days after, AUR at a dose of 2.5 mg/kg once a day and L-ASC at a dose of 3 g/kg twice a day were administered i.p. Treatment has been conducted for six days and then after two days of break drugs injections have been continued for additional six days. Control and single agent-treated mice received DMSO, as an AUR solvent, and NaCl at doses corresponding to  $\text{Na}^+$  from L-ASC salt. Tumor growth (left panel) was monitored two times per week by means of calipers. The mice were sacrificed when the tumors reached 15 mm of diameter. Survival of mice (right panel) was evaluated by Kaplan-Meier analysis. Statistical significance was determined using log-rank survival test; \*  $p < 0.05$ . The graphs represent results pooled from two independent experiments, number of mice in each group was 10.



**Supplementary Figure 8. Catalase abolishes L-ASC-mediated H<sub>2</sub>O<sub>2</sub> generation.** Cell culture medium was pre-incubated or not with CAT (100 µg/ml) for 30 min at 37°C, supplemented with 200 µM L-ASC, 0.5 µM AUR or the mixture of both compounds and incubated for indicated time points at 37°C. PY1 probe was added to the medium at 10 µM final concentration. The fluorescence was measured using the excitation wavelength 514 nm and emission wavelength 550 nm. The amount of generated H<sub>2</sub>O<sub>2</sub> was normalized to control (DMSO) and presented as means ± SD from two experiments (n=4). Statistical significance was assessed using 2-way ANOVA test between all experimental groups versus control and is indicated on the graph; \*\*p<0.01.





Samples		Concentration [μmol/l]		
Number	Name	D-ASC peak	L-ASC peak	Mean
1	L-ASC-1		207,8	239,9
2	L-ASC-2		290,7	
3	L-ASC-3		221,3	
4	control-1	n.d.		n.d.
5	control-2	n.d.		
6	D-ASC-1	182,3		161,7
7	D-ASC-2	128,9		
8	D-ASC-3	173,8		
9	DHA-1		358,4	361,3
10	DHA-2		364,3	

**Supplementary Figure 9. Intracellular uptake of various forms of ascorbate.** Raji cells were incubated with 500 μM L-ASC, D-ASC or L-DHA for 6h and then washed with PBS. The intracellular concentration of the compounds was assessed by HPLC as described in Supplementary methods. The representative HPLC chromatograms for control sample, L-ASC-, D-ASC- and L-DHA-containing samples are shown (left panel). The table presents the values of measured concentrations of control (n=2), L-ASC (n=3), D-ASC (n=3) and L-DHA (n=2) in Raji cells (right panel); n.d. – not detected.

	Control	15 min	1h	2h	4h	6h
Dose	2 g/kg					
Concentration [mM]	0,046	21,275	3,084	0,288	0,150	0,113
Standard deviation [mM]	0,009	5,634	1,468	0,063	0,030	0,017
Number of mice	n = 5	n = 5	n = 5	n = 5	n = 5	n = 5

	Control	15 min	1h	2h	4h	6h
Dose	4 g/kg					
Concentration [mM]	0,031	20,745	3,097	0,459	0,178	0,105
Standard deviation [mM]	0,022	10,056	1,470	0,137	0,071	0,054
Number of mice	n = 3	n = 2	n = 3	n = 3	n = 4	n = 4

**Supplementary Table 1. Pharmacokinetics of L-ASC.** L-ASC was administered i.p. at doses of 2 or 4 g/kg to BALB/c mice and the blood was collected from cheek vein after 15 min, 1 h, 2 h, 4 h, and 6 h. The concentration of L-ASC was assessed by HPLC, Dionex 3000 –ICS, as described in Supplementary methods.

# Supplementary Table 1

	Combination index (CI)			
	200 L-ASC + 0.25 AUR	200 L-ASC + 0.5 AUR	400 L-ASC + 0.25 AUR	400 L-ASC + 0.5 AUR
Raji	0.32	0.20	0.20	0.15
CI	0.39	0.26	0.53	0.31
	200 L-ASC + 0.125 AUR	200 L-ASC + 0.25 AUR	400 L-ASC + 0.125 AUR	400 L-ASC + 0.25 AUR
CLL38	0.67	0.63	0.91	0.94
CLL46	0.45	0.62	0.25	0.53
CLL61	0.39	0.25	0.52	0.31
CLL63	0.37	0.70	0.50	0.35
CLL66	0.62	0.56	0.68	0.62
CLL67	0.48	0.75	0.38	0.73
CLL68	0.40	0.22	0.29	0.10
CLL-G220	0.57	0.48	0.52	0.62
CLL-G324	0.76	0.56	0.60	0.56
CLL-G411	0.29	0.25	0.43	0.39

**Supplementary Table 2. Assessment of L-ASC and AUR combination effects.** The types of L-ASC and AUR interaction were calculated using CompuSyn software [7]. The resulting combination index (CI) indicates additive effect (CI = 1), synergism (CI < 1), or antagonism (CI > 1).

## Supplementary Table 2